Solid-State ^{13}C NMR Analyses of the Structure and Chain Conformation of Thermotropic Liquid Crystalline Polyurethane Crystallized from the Melt through the Liquid Crystalline State

Hiroyuki Ishida, Hironori Kaji, and Fumitaka Horii*

Institute for Chemical Research, Kyoto University, Uji, Kyoto 611, Japan

Received March 11, 1997; Revised Manuscript Received June 10, 1997[⊗]

ABSTRACT: Solid-state ^{13}C NMR analyses of the structure and chain conformation have been performed for a thermotropic liquid crystalline polyurethane that was polymerized from 3,3′-dimethyl-4,4′-biphenyldiyl diisocyanate, 1,10-decanediol, and 1-hexanol with a mole ratio of 25/24/2. This sample was crystallized by cooling from the isotropic melt through the liquid crystalline state at a rate of 1 °C/min. DSC thermograms of the cooling scan exhibit only one endothermic peak, whereas two exothermic peaks corresponding to the melting and isotropic points appear in the heating scan. However, the polarizing optical microscopic observation confirms that the crystallization occurs almost at the same time after the appearance of the liquid crystalline phase, although some part of the liquid crystalline phase is frozen without crystallization. T_{1C} analyses reveal that the sample contains three components with different T_{1C} values, which correspond to the crystalline, medium, and noncrystalline regions. From the line shape analyses of these three components, spacer methylene sequences for the crystalline and medium components are found to be in the same all *trans* conformation. In contrast, the methylene sequence for the noncrystalline component, which is ascribed to the frozen liquid crystalline component, is in the alternate *trans* and *trans−gauche* exchange conformation, probably reflecting the conformation that exists in the liquid crystalline state.

Introduction

Main-chain thermotropic liquid crystalline polymers, which basically consist of rigid mesogens and flexible spacers, produce different types of liquid crystalline states depending on the chemical structures of these constituent units as well as on the sorts of chemical bonds connecting the units. A large number of publications have already reported syntheses, structures, and properties of the liquid crystalline polymers.[1] More recent characterizations of the structure and chain conformation have been carried out by using different analytical methods such as X-ray diffractometry,[2−9] small angle neutron scattering,[4] transmission electron microscopy,[6,7,10] FT-IR spectroscopy,[11] solid-state ^{2}H NMR[12−14] and ^{13}C NMR[11,15,16] spectroscopies. Of these, high-resolution solid-state NMR spectroscopy is the most powerful method for characterizing the detailed structure and molecular motion of the respective constituent units. In particular, chain conformation, orientation, and intermolecular interactions such as hydrogen bonding can be well analyzed for the respective carbons or for other nuclei of the mesogens, spacers, and their connecting units in all possible states of liquid crystalline polymers.

We have recently characterized the crystalline−noncrystalline structure and hydrogen bonding as well as molecular motion for different solid polymers such as polyolefins,[17−20] polyether,[21] polyesters,[22,23] polyurethane,[24] poly(vinyl alcohol),[25−27] cellulose,[28−30] and so on, by mainly using high-resolution solid-state ^{13}C NMR spectroscopy. In this paper we apply a similar ^{13}C NMR analysis to the characterization of the chain conformation of the methylene spacer for a liquid crystalline polyurethane sample which was crystallized from the isotropic melt through the nematic liquid crystalline phase. First the contributions from different regions observed in CP/MAS ^{13}C NMR spectra are resolved into the respective spectra on the basis of the difference in ^{13}C spin−lattice relaxation times. Next the chain conformation of the spacer is evaluated in detail for each different region by considering the *γ-gauche* effect on the chemical shifts of methylene carbons. The orientation and molecular mobility of the mesogen group and the hydrogen bonding of the urethane bond will be reported in the following paper.

Chart 1

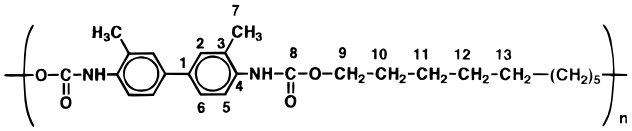

Experimental Section

Samples. 1,10-Decanediol and 1-hexanol were purchased from Nacalai Tesque in Kyoto and 3,3′-dimethyl-4,4′-biphenyldiyl diisocyanate was provided from Nippon Soda Co. Ltd. These materials were used without further purification.

The polyurethane sample PDBDM was polymerized in anisole at 140 °C for 6 h with 3,3′-dimethyl-4,4′-biphenyldiyl diisocyanate as the mesogen, 1,10-decanediol as the spacer, and 1-hexanol as the molecular weight controller in a molar ratio of 25/24/2.[31] The structure of the polymer is shown in Chart 1.

The number-average molecular weight, which was determined by the end-group analysis using solution-state ^{1}H NMR spectroscopy, was 11 700. This sample was crystallized under an argon atmosphere by cooling from 240 °C, which corresponds to the isotropic phase, through the liquid crystalline state at a rate of 1 °C/min.

Solid-State ^{13}C NMR Measurements. Solid-state ^{13}C NMR measurements were performed at room temperature on a JEOL JNM-GSX200 spectrometer equipped with a variable temperature MAS system operating at 50.0 MHz under a static magnetic field of 4.7 T. The sample was packed in a 7 mm cylindrical zirconia rotor. ^{1}H and ^{13}C radio-frequency field strengths $\gamma B_1/2\pi$ were 61.0−62.5 kHz. The contact time for the CP process was 2.0 ms and the recycle time after the acquisition of an FID was 5 s throughout this work. The MAS rate was set to 4.0 kHz to avoid the overlapping of spinning

[⊗] Abstract published in *Advance ACS Abstracts,* September 1, 1997.

S0024-9297(97)00326-4 CCC: $14.00 © 1997 American Chemical Society

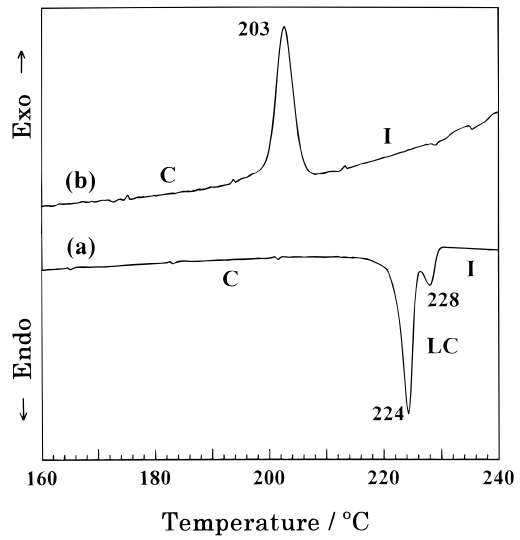

Figure 1. DSC thermograms of PDBDM crystallized from the melt by cooling at 1 °C/min: (a) heating at 2 °C/min; (b) cooling at 2 °C/min.

side bands on other resonance lines. The number of scans was usually 400. ^{13}C chemical shifts were expressed as values relative to tetramethylsilane (Me_4Si) by using the CH_3 line at 17.36 ppm of hexamethylbenzene crystals as an external reference. ^{13}C spin−lattice relaxation times (T_{1C}) were measured by using the CPT1 pulse sequence.[32]

Differential Scanning Calorimetry (DSC). The thermal transition behavior was measured by a TA Instruments DSC2910 differential scanning calorimeter. Indium was used as a standard for temperature calibration. All DSC runs were made for 1.6−2.7 mg samples under a nitrogen atmosphere with different heating or cooling rates. First-order transitions were read as maxima or minima of the endothermic or exothermic peaks.

Optical Microscopy. Thermal phase transitions and texture changes were observed with a Nikon OPTIPHOT2-POL optical polarizing microscope equipped with a Mettler FP-80/82 hot stage. Powder-like PDBDM was placed on a glass slide and covered with a glass cover slip. Each sample was heated or cooled under a nitrogen atmosphere in the hot stage at a fixed rate.

Results and Discussion

Thermal Transition Behavior. In order to confirm the existence of the liquid crystalline phase for the PDBDM sample, DSC measurements and polarizing optical microscopic observations have been performed. Figure 1 shows DSC heating and cooling thermograms for the PDBDM sample crystallized at a cooling rate of 1 °C/min. On the heating process at 2 °C/min, two exothermic peaks clearly appear as shown in Figure 1a. Furthermore, polarizing optical microscopic observations have confirmed that the liquid crystalline phase really forms in the temperature region between the two DSC peaks, as shown in Figure 2. In contrast, it is impossible to observe two corresponding endothermic peaks for the cooling process done at a conventional cooling rate of 1−5 °C/min, as shown in Figure 1b. It is, however, found by polarizing optical microscopy that the liquid crystalline phase first appears and then the crystallization follows immediately with decreasing temperature in the temperature region for the DSC endothermic peak, in concomitance with the further development of the liquid crystalline phase.

The polarizing optical microscopic observations during the cooling process also exhibited that the liquid crystalline formation occurs over the entire area of the

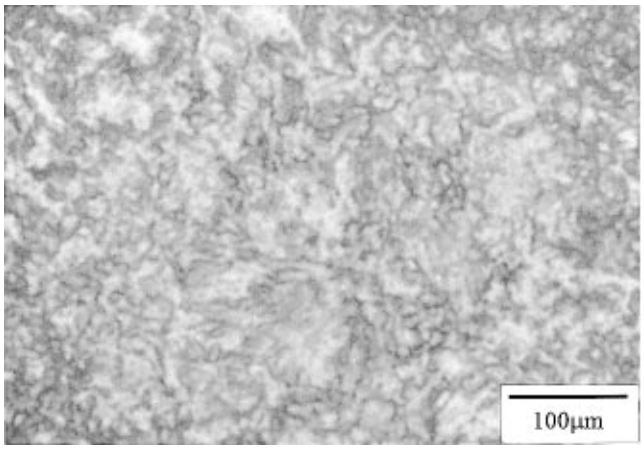

Figure 2. Polarizing optical microphotograph for PDBDM at 210 °C on cooling at 5 °C/min.

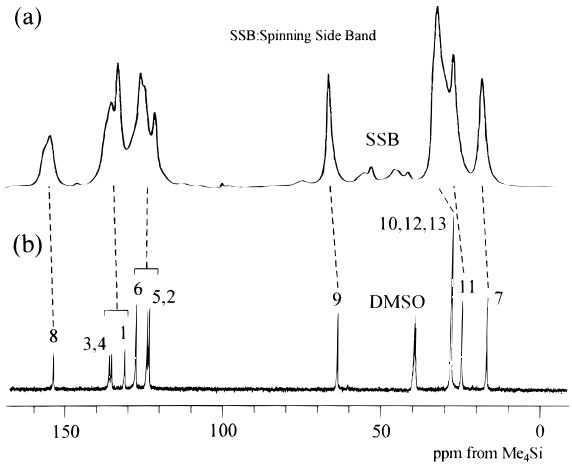

Figure 3. ^{13}C NMR spectra of PDBDM: (a) 50 MHz CP/MAS spectrum measured at room temperature; (b) 100 MHz solution state spectrum measured at 100 °C.

powder-like sample but that some parts of the liquid crystalline phase remain uncrystallized at room temperature. Such parts should be referred to as the frozen liquid crystalline phase.

CP/MAS ^{13}C NMR Spectrum. Figure 3a shows the CP/MAS ^{13}C NMR spectrum of the PDBDM sample measured at room temperature. The assignment of each resonance line has been made on the basis of the result for the solution state spectrum shown in Figure 3b. Here, the latter assignment was made separately from the INADEQUATE spectrum. As is clearly seen in Figure 3a, resonance lines ascribed to the carbonyl carbon, mesogen aromatic carbons, and spacer methylene carbons are well separated from each other. However, the crystalline and noncrystalline contributions are not straightforwardly observed as differences in chemical shift unlike the cases of polyethylene,[17,19,20] poly(tetramethylene oxide),[21] and poly(ϵ-caprolactone).[23]

^{13}C Spin−Lattice Relaxation Behavior. In order to examine the crystalline−noncrystalline structure of PDBDM, ^{13}C spin−lattice relaxation behavior has been measured at room temperature by the CPT1 pulse sequence.[32] In Figure 4 the logarithmic peak intensity of the C9 carbon is plotted against the decay time τ for the T_1 relaxation. Since the decay curve appears not to be a single exponential, it was analyzed in terms of multiple components, each having different T_{1C} values, by the computer-aided nonlinear least-squares method. The solid line is the result calculated by assuming three

Table 1. ^{13}C Spin−Lattice Relaxation Times of PDBDM Measured at Room Temperature

	T_{1C}/s								
	C8	C1,3,4		C,2,5,6		C9	C10,12,13	C11	C7
crystalline	210	217	233	243	201	217	227	191	160
medium	25.4	22.3	26.5	23.4	17.0	18.8	22.6	13.3	21.5
noncrystalline	3.3	0.49	0.47	3.3	0.60	0.95	1.0	0.48	4.3

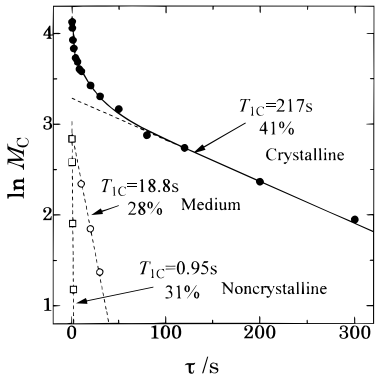

Figure 4. ^{13}C spin−lattice relaxation process for the C9 methylene carbon measured by the CPT1 pulse sequence.

components with different T_{1C} values, where the exponential decay of each component is also shown as a broken line. The experimental points agree well with the calculated curve, indicating the existence of three components with different T_{1C} values for the C9 line. Other resonance lines are also found to contain three components with T_{1C} values of similar orders, which are listed in Table 1.

The component with the longest T_{1C} values should be assigned to the crystalline component, because the existence of the crystalline component has been clearly confirmed by the X-ray diffraction method. On the other hand, the component with the shortest T_{1C} values can be assigned to the noncrystalline component. Although this component corresponds to the frozen liquid crystalline component, as described later, this assignment is used in this work to simply descriminate between the crystallized and notcrystallized materials. The component with intermediate T_{1C} values is simply called the medium component, because the content of this component is not well-known at present.

Spectra of the Three Components. Figure 5 shows ^{13}C NMR spectra of the crystalline, medium, and noncrystalline components for the methylene carbons, which are separately recorded by using the difference in T_{1C} as follows. The spectrum of the crystalline component has been selectively measured using the CPT1 pulse sequence[32] by setting the T_1 decay time τ to 100 s. The spectrum of the medium component has been obtained by subtracting the crystalline spectrum from the spectrum measured with the CPT1 pulse sequence by setting τ = 8 s. In these spectra, the noncrystalline component completely disappears due to the short T_{1C} values. As for the noncrystalline component, the spectrum has been measured by the saturation recovery method modified[17,21] for solid-state measurements by setting the T_1 recovery delay time to 2 s, although some minor contribution from the medium component is included in this spectrum, as described later.

The chemical shifts of the respective lines for the crystalline and medium components are in good accord with each other, indicating the same chain conformation for both components. Here, the relative intensities of the peaks are not exactly proportional to the composi-

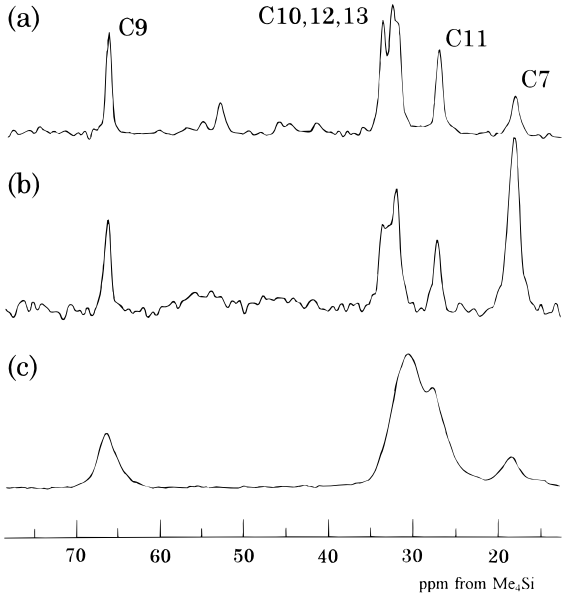

Figure 5. ^{13}C NMR spectra of different components of PDBDM: (a) the crystalline component; (b) the medium component; (c) the noncrystalline component.

tions of the respective carbons due to the difference in T_{1C}. In contrast, the resonance lines of the noncrystalline component are rather broad, possibly due to higher molecular mobility and wider distributions in local structure. More interestingly, the C10, C12, and C13 resonance lines significantly shift upfield compared to the corresponding lines of the crystalline and medium components, whereas the C9 and C11 lines stay constant.

We intend to interpret such upfield shifts in terms of the so-called *γ-gauche* effect.[33] The *γ-gauche* effect is the conformational effect on chemical shifts of the successive C−C−C−X sequence. In the case of the methylene sequence $C^0-C^\alpha-C^\beta-C^\gamma$, carbon C^0 and its γ-substituent methylene carbon C^γ are separated by three intervening bonds, and their mutual distance and orientation are variable depending on the conformation of the central bond $C^\alpha-C^\beta$. Therefore, the change in the conformation of the $C^\alpha-C^\beta$ bond brings about the variation in the electron shielding of C^0 by C^γ; the *gauche* conformation in the bond induces about 5 ppm upfield shift compared to the *trans* conformation.

Line shape analyses have been carried out for the spectra of the crystalline and noncrystalline components shown in Figure 5a,c. Figure 6 shows the result of the computer line shape analysis for the spectrum of the crystalline component. Here, each line is assumed to be described by a Lorentzian curve. It is clearly found that the resonance lines located at 35−30 ppm are well resolved into three Lorentzian curves, which correspond to the resonance lines for C10, C12, and C13 carbons.

On the basis of the chemical shifts of the C10, C12, and C13 carbons determined for the crystalline component in Figure 6, a similar line shape analysis has been conducted for the spectrum of the noncrystalline component. In this analysis the following two assumptions

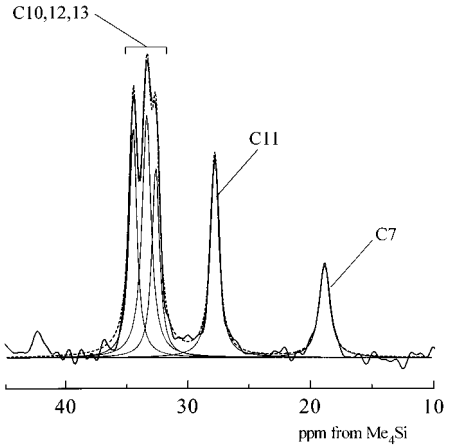

Figure 6. Line shape analysis for the methylene resonance lines of the crystalline component.

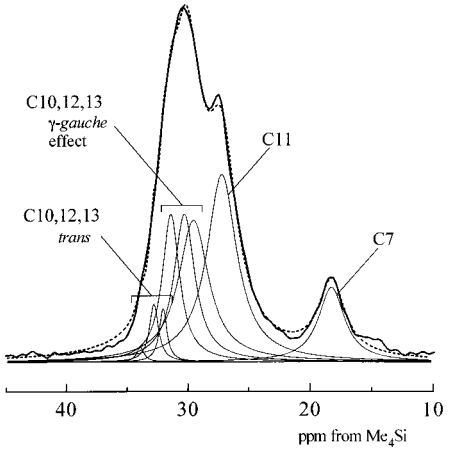

Figure 7. Line shape analysis for the methylene resonance lines of the noncrystalline component.

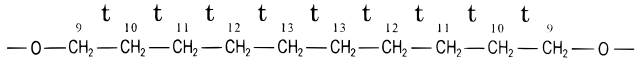

(a)

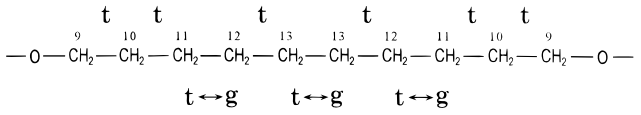

(b)

Figure 8. Conformations for the methylene sequences in different components in PDBDM: (a) crystalline and medium components; (b) noncrystalline component (frozen liquid crystalline component).

were made: (1) the methylene carbons of the crystalline component have the all *trans* conformation; (2) the upfield shift of the ^{13}C chemical shift value due to the *γ-gauche* effect is half (2.5 ppm) of the conventional value (5 ppm).[33] The former assumption is highly reasonable because there are previous reports[15,16] for main-chain thermotropic liquid crystalline polymers that support this assumption. As for the second assumption, a detailed discussion will be made later.

Figure 7 shows the best result of the computer line shape analysis for the spectrum of the noncrystalline component performed under those assumptions. On the downfield side, the minor contributions indicated by the three Lorentzians correspond to the resonance lines of C10, C12, and C13 carbons of the medium component.

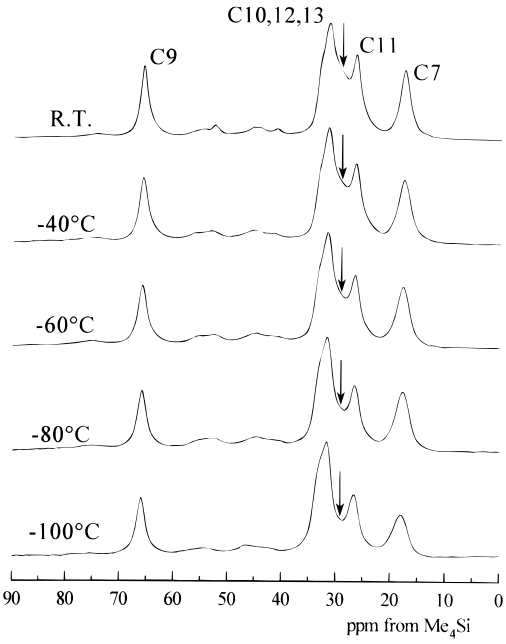

Figure 9. 50 MHz ^{13}C CP/MAS NMR spectra of PDBDM measured at various temperatures.

These peaks appear in this spectrum because the T_{1C} values of the medium component are not so long compared to those of the noncrystalline component. The other three Lorentzian curves around 30 ppm are ascribed to the C10, C12, and C13 lines which undergo 2.5 ppm upfield shifts due to the *γ-gauche* effect. Moreover, the two most upfield peaks should be the contributions from the C11 and C7 carbons. The composite curve of these eight Lorentzians, which is indicated by a broken line, is in good accord with the experimental spectrum indicated by a thick solid line. It is, therefore, concluded that the noncrystalline lines of the C10, C12, and C13 carbons are subjected to the *γ-gauche* effect with a 2.5 ppm upfield shift, suggesting that some *gauche* conformations exist in the methylene sequence.

According to this conclusion, the most probable conformations for the methylene sequences in different components are illustrated in Figure 8. As for the noncrystalline component, the *gauche* conformation should be introduced to the C11−C12 and C13−C13 bonds to explain the *γ-gauche* effect on the C10, C12, and C13 carbons. Moreover, since the upfield shift due to the *γ-gauche* effect is half of the conventional value, it indicates that rapid exchange occurs between the *trans* and *gauche* conformations around these C−C bonds. Such a characteristic conformation should be referred to as the alternate *trans* and rapid *trans*−*gauche* exchange conformation.

Yoon et al.[12,34] proposed similar alternate *trans* conformations for the methylene spacers of main-chain liquid crystalline polymers on the basis of thermodynamic simulations. Their recent ^{2}H NMR study[13,14] also revealed that the methylene spacer of a thermotropic liquid crystalline polyether adopts the alternate *trans* and rapid *trans*−*gauche* exchange conformation. Our finding in the frozen nematic phase is basically in good accord with these previous results. Nevertheless, one difference should be noted here; the terminal C−C bonds (the C9−C10 bonds) adopt the *trans* conformation instead of the *trans*−*gauche* exchange conformation, as shown in Figure 8. This fact may be associated with

the features of the urethane bond or the frozen nematic phase.

To obtain further information on the spacer conformation, CP/MAS ^{13}C NMR measurements were performed at lower temperatures. Figure 9 shows the CP/MAS ^{13}C NMR spectra of PDBDM at various temperatures, which contain contributions from all of the three components described above. The contribution from the noncrystalline component for the C10, C12, and C13 carbons appears at room temperature at around 30 ppm, as is indicated by an arrow in the figure, owing to the upfield shift caused by the *γ-gauche* effect. However, interestingly enough, this noncrystalline contribution is greatly reduced in intensity with decreasing temperature, and this reduction of the intensity is induced by the downfield shift of the noncrystalline resonance lines. This fact evidently indicates that, at low temperatures, the *trans*−*gauche* exchange conformation becomes fixed in the *trans* conformation even in the noncrystalline region. Since this change in conformation with temperature is found to be a reversible process, it is hypothesized that some orientational factor of the mesogen group and the urethane bond prevents the fixation of the *trans* conformation. Similar detailed characterizations are in progress for the mesogen group and the urethane bond to clarify the effects of these structural units.

References and Notes

(1) For example: (a) Ciferri, A., Ed. *Liquid Crystalline Polymers. Principles and Fundamental Properties*; VCH Publishers: New York, 1991. (b) Collyer, A. A., Ed., *Liquid Crystal Polymers: From Structure to Applications*; Polymer Liquid Crystals Series 1; Chapman & Hall: London, 1992. (c) Carfagna, C., Ed. *Liquid Crystalline Polymers*; Pergamon: Oxford, U.K., 1994. (d) Acierno, D., Collyer, A. A., Eds. *Rheology and Processing of Liquid Crystalline Polymers*; Polymer Liquid Crystal Series 2; Chapman & Hall: London, 1996.

(2) Han, C. D.; Chang. S.; Kim, S. S. *Macromolecules* **1994**, *27*, 7699.

(3) Li, X.; Brisse, F. *Macromolecules* **1994**, *27*, 7725.

(4) Hardouin, F.; Sigaud, G.; Achard, M. F.; Brûlet, A.; Cotton, J. P.; Yoon, D. Y.; Percec, V.; Kawasumi, M. *Macromolecules* **1995**, *28*, 5427.

(5) Francescangeli, O.; Yang, B.; Laus, M.; Angeloni, A. S.; Galli, G.; Chiellini, E. *J. Polym. Sci., Part B: Polym. Phys.* **1995** *33*, 699.

(6) Yoon, Y.; Zhang, A.; Ho, R.-M.; Cheng, S. Z. D.; Percec, V.; Chu, P. *Macromolecules* **1996**, *29*, 294.

(7) Yoon, Y.; Ho, R.-M.; Moon, B.; Kim, D.; McCreight, K. W.; Li, F.; Harris, F. W.; Cheng, S. Z. D.; Percec, V.; Chu, P. *Macromolecules* **1996**, *29*, 3421.

(8) Tokita, M.; Takahashi, T.; Mayashi, M.; Inomata, K.; Watanabe, J. *Macromolecules* **1996**, *29*, 1345.

(9) Langelaan, H. C.; Boer, A. P. *Polymer* **1996**, *37*, 5667.

(10) Wegner, G. *Macromol. Symp.* **1996**, *101*, 257.

(11) Silvestri, R. L.; Koenig, J. L. *Polymer* **1994**, *35*, 2528.

(12) Bruckner, S.; Scott, J. C.; Yoon, D. Y.; Griffin, A. C. *Macromolecules* **1985**, *18*, 2709.

(13) Sherwood, M. H.; Sigaud, G.; Yoon, D. Y.; Wade, C. G.; Kawasumi, M.; Percec, V. *Mol. Cryst. Liq. Cryst.* **1994**, *254*, 455

(14) Leisen, J.; Boeffel, C.; Spiess, H. W.; Yoon, D. Y.; Sherwood, M. H.; Kawasumi, M.; Percec, V. *Macromolecules* **1995**, *28*, 6937.

(15) Cheng, J.; Jin, Y.; Wunderlich, B.; Cheng, S. Z. D.; Yandrasits, M. A.; Zhang, A.; Percec, V. *Macromolecules* **1992**, *25*, 5991.

(16) Cheng, J.; Jin, Y.; Chen, W.; Wunderlich, B.; Jonsson, H.; Hult, A.; Gedde, U. W. *J. Polym. Sci., Part B: Polym. Phys.* **1994**, *32*, 721.

(17) Kitamaru, R.; Horii, F.; Murayama, K. *Macromolecules* **1986**, *19*, 639.

(18) Saito, S.; Moteki, Y.; Nakagawa, M.; Horii, F.; Kitamaru, R. *Macromolecules* **1990**, *23*, 3257.

(19) Kimura, T.; Neki, K.; Tamura, N.; Horii, F.; Nakagawa, M.; Odani, H. *Polymer* **1992**, *33*, 493.

(20) Kitamaru, R.; Horii, F.; Zhu, Q.; Bassett, D. C.; Olley, R. H. *Polymer* **1994**, *35*, 1171.

(21) Hirai, A.; Horii, F.; Kitamaru, R.; Fatou, J. G.; Bello, A. *Macromolecules* **1990**, *23*, 2913.

(22) Tsuji, H.; Horii, F.; Nakagawa, M.; Ikada, Y.; Odani, H.; Kitamaru, R. *Macromolecules* **1992**, *25*, 4114.

(23) Kaji, H.; Horii, F. *Macromolecules*, in press.

(24) Ishida, M.; Yoshinaga, K.; Horii, F. *Macromolecules* **1996**, *29*, 8824.

(25) Horii, F.; Hu, S.; Ito, T.; Odani, H.; Matsuzawa, S.; Yamaura, K. *Polymer* **1992**, *33*, 2299.

(26) Hu, S.; Tsuji, M.; Horii, F. *Polymer* **1994**, *35*, 2516.

(27) Horii, F.; Masuda, K.; Kaji, H. *Macromolecules* **1997**, *30*, 2519.

(28) Yamamoto, H.; Horii, F. *Macromolecules* **1993**, *26*, 1313.

(29) Yamamoto, H.; Horii, F. *Cellulose* **1994**, *1*, 57.

(30) Yamamoto, H.; Horii, F.; Hirai, A. *Cellulose* **1996**, *3*, 229.

(31) Iimura, K.; Koide, N.; Tanabe, H.; Takeda, M. *Macromol. Chem.* **1981**, *182*, 2569.

(32) Torchia, D. A. *J. Magn. Reson.* **1981**, *44*, 117.

(33) Tonelli, A. E. *NMR Spectroscopy and Polymer Microstructure: The Conformational Connection*; VCH Publishers: New York, 1989.

(34) Yoon, D. Y.; Bruckner, S. *Macromolecules* **1985**, *18*, 651.

MA9703261